

Electric-field driven flat bands in the distorted sawtooth chain via the Katsura-Nagaosa-Balatsky mechanism

Vadim Ohanyan,^{1,2} Lusik Amiraghyan,^{1,3} Michael Sekania,^{4,5} and Marcus Kollar⁶

¹Laboratory of Theoretical Physics Yerevan State University, 1 Alex Manoogian Str., 0025 Yerevan, Armenia

²CANDLE, Synchrotron Research Institute, 31 Acharyan Str., 0040 Yerevan, Armenia

³Institute of Applied Problems of Physics, 25 Hr. Nersisyan St, Yerevan 0014, Armenia

⁴Rechenzentrum, University of Augsburg, 86135 Augsburg, Germany

⁵Andronikashvili Institute of Physics, Javakishvili Tbilisi State University, Tamarashvili str. 6, 0177 Tbilisi, Georgia

⁶Theoretical Physics III, Center for Electronic Correlations and Magnetism, Institute of Physics, University of Augsburg, 86135 Augsburg, Germany

(Dated: December 2, 2025)

We investigate flat magnonic bands in a generalized sawtooth-chain model in which three sets of exchange parameters (symmetric Heisenberg exchange, axial Ising anisotropy, and antisymmetric Dzyaloshinskii-Moriya (DM) exchange) are assigned independently to each side of the triangular plaquette. If the effective Dzyaloshinskii-Moriya (DM) interaction parameters are generated via the Katsura-Nagaosa-Balatsky (KNB) mechanism of magnetoelectricity, they become explicit functions of the electric-field magnitude and direction, as well as of the lattice geometry, which in the present case is characterized by two bond angles. We focus on the situation in which these two angles are unequal, corresponding to a distortion of the triangular plaquette. Several electric-field induced flat-band scenarios in the distorted sawtooth chain are analyzed, and expressions are derived for the electric-field strength required to drive the one-magnon excitations into a flat-band regime when the field is aligned along the lattice bonds. The saturation field and its dependence on the distortion angle are also examined. Finally, we establish a mapping between the flat-band solutions for a general DM interaction and its specific KNB-induced form.

This article is dedicated to the memory of Johannes Richter.

PACS numbers: 71.10.-w, 75.10.Lp, 75.10.Jm

Keywords: Sawtooth chain, KNB mechanism, Magnetoelectric effect, Localized magnons, Flat bands

I. INTRODUCTION

Localization in many-body quantum models continues to be a focus of numerous researches. The most extensively studied many-body quantum models exhibiting well-understood localized states are tight-binding models, or quantum lattice models with mobile non-interacting particles [1–5]. The first evidence for dispersionless single-particle eigenstates in a two-dimensional tight-binding Hamiltonian appeared in the 1980s [6]. Shortly thereafter, the analysis of special lattice topologies within the Hubbard model framework led to the prediction of interaction-driven ferromagnetism at half-filling, even for finite on-site repulsion U [7–13]. More recent developments have described the paramagnetic-to-ferromagnetic transition in flat-band Hubbard systems in terms of Pauli-correlated percolation [11–13]. In the past decades, significant experimental progress was made in realizing flat-band physics in photonic lattices [14–16], ultracold atoms in optical lattices [17–19], twisted bilayer graphene [20, 21], and other topological flat-band materials [22, 23]. By contrast, Heisenberg and other quantum spin Hamiltonians are intrinsically strongly interacting systems, and localized states in such translationally invariant spin models might initially appear to belong to the class of many-body localized (MBL) states. Indeed, MBL physics is well-established in disordered one-dimensional quantum spin models [24]. However, the

phenomenon of localized magnons in frustrated magnets shares many conceptual similarities with flat-band localization in tight-binding systems [25–31]. Among the various excitations in quantum spin models the magnonic excitations are special, in that they occur as low-lying quasi-particle excitation above a saturated state in the spectrum of all such models. When the magnetic field magnitude is close to and below the saturation field the main magneto-thermal properties of the system can be captured by the model of non-interacting magnons, which has the form of a tight-binding model. The corresponding Hamiltonian can be constructed within linear spin-wave theory in terms of the Holstein-Primakoff transformation [31]. Alternatively, for each quantum-spin lattice model it is straightforward to construct a one-magnon state, as a translationally invariant superposition of $S_j^- |0\rangle$, where $|0\rangle = |S, S, \dots, S\rangle$ is the reference polarized or ferromagnetic state, a direct product of $S^z = S$ spin states at each sites of the lattice. The eigenvalues of the Hamiltonian for such a states are the branches of the exact one-magnon spectrum, with the number of branches corresponding to the number of the site in the unit cell. A number of lattice spin models demonstrating localized magnons are known in all dimensions [1]. However, almost all of them demand additional constraints for the exchange constants of the model, transforming the lower band of the one-magnon spectrum into a flat one. One of the simplest quantum spin chains which admit localized

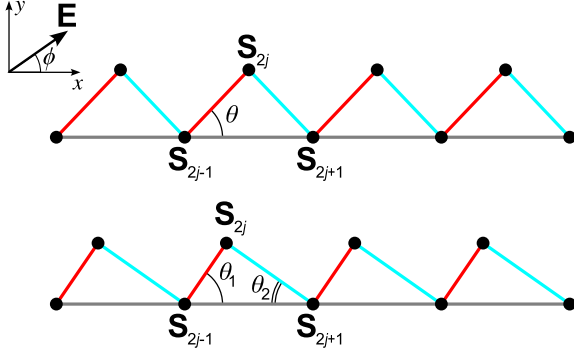


FIG. 1. (Color online) Symmetric and distorted sawtooth chains with three different coupling(s) for each side of triangle. The filled circles show the lattice sites occupied by spins. The exchange coupling, the XXZ anisotropy and DM interaction along the basal line (black) are J_1 , Δ_1 and D_1 , respectively. Left (red) and right (blue) bonds along the zigzag line feature the parameters J_2 , Δ_2 and D_2 (red) and J_3 , Δ_3 and D_3 (blue), respectively. The symmetric case features the same bond angles θ for the left and right bonds of the triangle, while in the distorted chain they are θ_1 and θ_2 , respectively. The basal line is chosen to be parallel to x -axis and electric field vector lies in (x, y) plane.

magnons is the sawtooth chain [1, 25–31], which is a chain of corner-sharing triangles (see Fig. 1). The XXZ model on the sawtooth chain with two exchange couplings, J_1 for the basal line and J_2 for the zigzag part, exhibits a flat band if

$$J_2 = \pm \sqrt{2(1 + \Delta_1)} J_1, \quad (1.1)$$

where Δ_1 is the axial exchange anisotropy for the basal line [25]. However, this restriction can be overcome with the aid of electric field [30, 31] in the sawtooth chain by a special type of magnetoelectric coupling, the Katsura-Nagaosa-Balatsky (KNB) mechanism [32–35]. It was shown in Ref. [30] that in the sawtooth chain with two exchange couplings and no axial anisotropy ($\Delta_1 = 1$), the lower branch of the one-magnon spectrum becomes flat when electric field is pointed along the basal line and its magnitude is given by

$$E_{FB} = \pm \frac{\sqrt{4J_1^2 - J_2^2}}{\sin \theta}. \quad (1.2)$$

This result is quite remarkable, as it applies to arbitrary values of the exchange constants, provided $4J_1^2 > J_2^2$. Here θ is the angle between the basal line and zigzag

bonds in case of isosceles triangles. The KNB mechanism and an external in-plane electric field induce additional Dzyaloshinskii-Moriya (DM) interactions, which in general are different for the three sides of the triangle. The values of this induced DM exchange depend on the electric field magnitude E , its angle with the basal line ϕ and the lattice bond angle θ . Further developments of the ideas and results of Ref. [30] were presented in Ref. [31], where the generalized model of an XXZ sawtooth chain with three symmetric exchange couplings and three DM interactions was considered. The flat-band constraints derived in Ref. [31] are a system of two rational equations supplemented with an additional conditions of band ordering. The number of parameters involved in the constraints is seven, namely three symmetric exchange coupling, three DM parameters, and the axial anisotropy on the basal line. Therefore, a number of possible solution schemes were considered in Ref. [31]. Each scheme offers a solution in terms of two or three quantities out of seven, when the remaining six or five are assumed to be given. Particularly interesting was a case for which the three DM parameters were given in terms of three symmetric exchange couplings and the axial anisotropy on the basal line. Parametrized by one continuous parameter, an infinite number of flat-band solutions was obtained. Moreover, it was also shown in Ref. [31] how to obtain flat-band solutions in terms of DM parameters induced by the KNB mechanism, i.e., by tuning the angle and the magnitude of the electric field. Nowadays, research on various aspects of spin ordering and one-magnon dynamics in the sawtooth chain with inhomogeneous couplings remains very active [36–41].

In the present paper we continue our investigations into the nature and features of the electric-field driven flat bands in the sawtooth chain. We generalize the model, considering now the sawtooth chain with distorted triangles. Namely the angles at the base line of the triangle, θ_1 and θ_2 , are different (see Fig. 1), which arises naturally from unequal length of these bonds. Our main finding is that, compared to the bond-symmetric case [30], a flat band can be induced with more flexibility in the case of $\theta_2 \neq \theta_1$, as detailed below.

II. THE MODEL AND KNB POLARIZATION

As in our previous paper [31] here we deal with the model of an XXZ sawtooth chain with DM interaction and three sets of interaction parameters, one for each side of triangle. The Hamiltonian thus has the following form,

$$\begin{aligned}
\mathcal{H} = & \sum_{j=1}^{N/2} \left(\frac{J_1 + iD_1}{2} S_{2j-1}^+ S_{2j+1}^- + \frac{J_1 - iD_1}{2} S_{2j-1}^- S_{2j+1}^+ + J_1 \Delta_1 S_{2j-1}^z S_{2j+1}^z \right) \\
& + \sum_{j=1}^{N/2} \left(\frac{J_2 + iD_2}{2} S_{2j-1}^+ S_{2j}^- + \frac{J_2 - iD_2}{2} S_{2j-1}^- S_{2j}^+ + J_2 \Delta_2 S_{2j-1}^z S_{2j}^z \right) \\
& + \sum_{j=1}^{N/2} \left(\frac{J_3 + iD_3}{2} S_{2j}^+ S_{2j+1}^- + \frac{J_3 - iD_3}{2} S_{2j}^- S_{2j+1}^+ + J_3 \Delta_3 S_{2j}^z S_{2j+1}^z \right) - B \sum_{j=1}^N S_j^z,
\end{aligned} \tag{2.3}$$

where S_j^α , $\alpha = x, y, z$ and $S_j^\pm = S_j^x \pm iS_j^y$ stand for the standard $SU(2)$ generators with $[S_j^\alpha, S_{j'}^\beta] = \delta_{jj'} \epsilon^{\alpha\beta\gamma} S_j^\gamma$. In order to have conservation of $S_{tot}^z = \sum_{j=1}^N S_j^z$, the direction of the Dzyaloshinskii vector coincides with the direction of the magnetic field. As mentioned above, the spin-induced ferroelectricity scheme of the KNB mechanism leads to DM terms, as the microscopic polarization of the bond between two spin [32] can be expressed as

$$\mathbf{P}_{j,j+1} = \gamma_{j,j+1} \mathbf{e}_{j,j+1} \times (\mathbf{S}_j \times \mathbf{S}_{j+1}), \tag{2.4}$$

where $\mathbf{e}_{j,j+1}$ is the unit vector pointed from site j to the site $j+1$ and $\gamma_{j,j+1}$ is a constant depending on the local features of the chemical bonds. The polarization appears due to a complicated redistribution of the electron density between two magnetic ions and the p -element atom in between which is covalently bonded to them[32–35]. The KNB polarization of the model includes an additional contribution to the Hamiltonian when an external electric field is applied,

$$\mathcal{H}_P = -\mathbf{E} \cdot \sum_{(i,j)} \gamma_{i,j} \mathbf{e}_{i,j} \times (\mathbf{S}_i \times \mathbf{S}_j). \tag{2.5}$$

Clearly this Hamiltonian can be represented in a general DM form,

$$\begin{aligned}
\mathcal{H}_P &= \sum_{(i,j)} \mathbf{D}_{i,j}(\mathbf{E}) \cdot (\mathbf{S}_i \times \mathbf{S}_j), \\
\mathbf{D}_{i,j}(\mathbf{E}) &= -\gamma_{ij} (\mathbf{E} \times \mathbf{e}_{ij}).
\end{aligned} \tag{2.6}$$

Here the electric-field dependent DM vector $\mathbf{D}_{i,j}(\mathbf{E})$ can be chosen parallel to the z -axis for the entire lattice, provided it is planar, i.e., for all bonds

$$\mathbf{e}_{ij} = A_{ij} \mathbf{e}_x + B_{ij} \mathbf{e}_y \tag{2.7}$$

and the electric field vector then lies in the same plane. Thus in order to obtain a quantum spin model with conserved S_{tot}^z , only special 1d and 2d lattices can be considered. The simplest case is a linear chain leading to

[42–49]

$$P^x = 0 \tag{2.8}$$

$$P^y = \gamma \sum_{j=1}^N (S_j^y S_{j+1}^x - S_j^x S_{j+1}^y)$$

$$P^z = \gamma \sum_{j=1}^N (S_j^z S_{j+1}^x - S_j^x S_{j+1}^z).$$

The next example is the spin chain folded to a regular zigzag structure, for which $\mathbf{e}_j = \cos \theta \mathbf{e}_x + (-1)^{j-1} \sin \theta \mathbf{e}_y$ and thus [30, 31, 50–53]

$$-\mathbf{E} \cdot \mathbf{P} \tag{2.9}$$

$$= \sum_{j=1}^N (E_y \cos \theta + (-1)^j E_x \sin \theta) (S_j^x S_{j+1}^y - S_j^y S_{j+1}^x).$$

Here the constant γ is absorbed into the definition of renormalized electric field components, E_x and E_y , measured in appropriate units. The symmetric sawtooth chain ($\theta_2 = \theta_1$) contains both a linear chain and a zigzag part, thus in this case the interaction between in-plane electric field and KNB polarization has the following form [30],

$$-\mathbf{E} \cdot \mathbf{P} \tag{2.10}$$

$$\begin{aligned}
&= \sum_{j=1}^N (E_y \cos \theta + (-1)^j E_x \sin \theta) (S_j^x S_{j+1}^y - S_j^y S_{j+1}^x) \\
&+ a E_y \sum_{j=1}^{N/2} (S_{2j-1}^x S_{2j+1}^y - S_{2j-1}^y S_{2j+1}^x).
\end{aligned}$$

The coefficient a here accounts for the possible difference in the microscopic features of the KNB mechanism for the bonds in the basal line and the zigzag part of the chain. It is easy to see that in case of an in-plane electric field, the interaction induced by the KNB polarization contributes a DM-type interaction as in Eq. (2.3) with

$$D_1 = aE \sin \phi, \tag{2.11}$$

$$D_2 = E \sin(\phi - \theta),$$

$$D_3 = E \sin(\phi + \theta),$$

where ϕ is the angle between the electric field and the basal line (x axis) of the chain. This case was analyzed

in detail in Ref. [30] and [31]. Finally for the distorted sawtooth chain (see Fig. 1), which we analyze in the following, the KNB mechanism for an in-plane electric field gives a Hamiltonian of the form (2.3) with DM parameters given by

$$\begin{aligned} D_1 &= aE \sin \phi, \\ D_2 &= E \sin(\phi - \theta_1), \\ D_3 &= E \sin(\phi + \theta_2), \end{aligned} \quad (2.12)$$

The general flat-band constraints derived and analyzed in Ref. [31] still apply. However now the connection between DM parameters and electric field is more complicated and contains an additional parameter, the deformation angle of the sawtooth chain. We note that models of the KNB mechanism in 2d and 3d magnets have also been in focus recently [54–56].

III. FLAT-BAND CONSTRAINTS AND GENERAL SOLUTIONS

As the flat-band constraints and the properties of their solution do not depend on the magnitude of spin, we therefore without loss of generality consider here only the case $S = 1/2$. The one-magnon spectrum and the corresponding flat-band constraints obtained in [31] are

$$\begin{aligned} \varepsilon_1^\pm(k) &= B - \frac{1}{2} \sum_{a=1}^3 J_a \Delta_a + \frac{1}{2} \rho_1 \cos(k - \phi_1) \\ &\pm \frac{1}{2} \left[(J_1 \Delta_1 - \rho_1 \cos(k - \phi_1))^2 \right. \\ &\quad \left. + 2\rho_2 \rho_3 \cos(k - \phi_2 - \phi_3) + \rho_2^2 + \rho_3^2 \right]^{\frac{1}{2}}, \end{aligned} \quad (3.13)$$

and

$$\begin{aligned} \phi_1 &= \phi_2 + \phi_3 \pm \pi \delta_{\sigma, -1}, \\ 0 &= \rho_1^2 (\rho_2^2 + \rho_3^2) + 2\sigma J_1 \Delta_1 \rho_1 \rho_2 \rho_3 - \rho_2^2 \rho_3^2, \\ \sigma &= \text{sign} \left(1 + \frac{D_1 D_2}{J_1 J_2} \right) \equiv \text{sign} \left(1 + \frac{D_1 D_3}{J_1 J_3} \right) \\ &\equiv \text{sign} \left(1 - \frac{D_2 D_3}{J_2 J_3} \right) = 1 \end{aligned} \quad (3.14)$$

respectively, where the following notations were adopted,

$$\begin{aligned} J_a + iD_a &= \rho_a e^{i\phi_a}, \quad \rho_a = \sqrt{J_a^2 + D_a^2}, \\ \phi_a &= \arctan \frac{D_a}{J_a}, \end{aligned} \quad (3.15)$$

After the substitution of the solution of flat-band constraints given in Eq. (3.14), the one-magnon spectrum (3.13) takes the following form:

$$\begin{aligned} \varepsilon_1^+(k) &= B - E_0 + \rho_1 \cos(k - \phi_1), \\ \varepsilon_1^-(k) &= B - B_0, \end{aligned} \quad (3.16)$$

where

$$\begin{aligned} E_0 &= \frac{1}{2} \left(2J_1 \Delta_1 + J_2 \Delta_2 + J_3 \Delta_3 - \frac{\rho_2 \rho_3}{\rho_1} \right), \\ B_0 &= \frac{1}{2} \left(J_2 \Delta_2 + J_3 \Delta_3 + \frac{\rho_2 \rho_3}{\rho_1} \right), \end{aligned} \quad (3.17)$$

and B_0 is the magnetic saturation field. The last condition in Eqs. (3.14) guarantees that the flat band lies below the dispersive one. Formally the flat-band constraints are a system of two rational equations for seven parameters, $J_1, J_2, J_3, D_1, D_2, D_3$ and Δ_1 . Hence there is a broad variety of possible solutions, several classes of which were analyzed in Ref. [31]. Solutions which are given in terms of the three DM constants are particularly interesting as they make a direct link with the electric-field driven flat band discussed in Ref. [30]. In that case one can express all three DM couplings in terms of the other Hamiltonian parameters in the following way,

$$\begin{aligned} D_1 &= \mp J_1 \frac{2J^2 \alpha (1 + \alpha) \sqrt{\frac{1}{\alpha} + \frac{W_\mu(\alpha)}{2J^2 \alpha^2}}}{W_\mu(\alpha)}, \\ D_2 &= \pm J_2 \sqrt{\frac{1}{\alpha} + \frac{W_\mu(\alpha)}{2J^2 \alpha^2}}, \\ D_3 &= \pm J_3 \alpha \sqrt{\frac{1}{\alpha} + \frac{W_\mu(\alpha)}{2J^2 \alpha^2}}, \end{aligned} \quad (3.18)$$

where

$$J = \frac{J_2 J_3}{J_1}, \quad (3.19)$$

$$\begin{aligned} W_\mu(\alpha) &= R(\alpha) + \mu \sqrt{R^2(\alpha) + 4J^2 \alpha (1 + \alpha) (J_2^2 + \alpha J_3^2)}, \\ R(\alpha) &= J_2^2 + \alpha^2 J_3^2 - 2\alpha \xi \Delta_1 J_2 J_3, \\ \mu &= \{-1, 1\}. \end{aligned}$$

Taking into account the square roots and the condition for ordering of the bands we obtain an additional constraint for the function $W_\mu(\alpha)$,

$$\begin{aligned} \alpha > 0, \quad W_\mu(\alpha) &\in (-2J^2 \alpha, 0), \\ \alpha < 0, \quad W_\mu(\alpha) &\in (0, -2J^2 \alpha). \end{aligned} \quad (3.20)$$

As $W_1(\alpha)$ is more likely to be positive and $W_{-1}(\alpha)$ negative, it is easier to find flat bands with $\text{sign}(\mu\alpha) = -1$, although the other case is still possible. To simplify the situation we consider the important particular case of homogeneous symmetric exchange parameters, $J_1 = J_2 = J_3 = J = 1$ and $\Delta_1 = \pm 1$, for which the DM parameters given in Eq. (3.19) for become

$$\begin{aligned} D_1 &= \mp \frac{2\alpha (1 + \alpha) \sqrt{\frac{1}{\alpha} + \frac{X_\mu(\alpha)}{2\alpha^2}}}{X_\mu(\alpha)}, \\ D_2 &= \pm \sqrt{\frac{1}{\alpha} + \frac{X_\mu(\alpha)}{2\alpha^2}}, \\ D_3 &= \pm \alpha \sqrt{\frac{1}{\alpha} + \frac{X_\mu(\alpha)}{2\alpha^2}}, \end{aligned} \quad (3.21)$$

where

$$X_\mu(\alpha) = \begin{cases} (1-\alpha)^2 + \mu\sqrt{(1-\alpha)^4 + 4\alpha(1+\alpha)^2}, & \Delta_1 = 1, \\ (1+\alpha)^2 + \mu\sqrt{(1+\alpha)^4 + 4\alpha(1+\alpha)^2}, & \Delta_1 = -1. \end{cases} \quad (3.22)$$

Here an additional constraint restricting the possible values of α (for given values of μ) must be imposed here ensure a positive value of the radicand. For $\Delta_1 = 1$ only $\mu = 1$ and $\alpha < 0$ are acceptable, in which case the radicand in Eq. (3.22) is always positive. For the case $\Delta_1 = -1$ both signs of μ can be compatible with the flat bands condition, however, α still must be negative, and there is an additional forbidden range

$$\alpha \in (-3 - 2\sqrt{2}, -3 + 2\sqrt{2}). \quad (3.23)$$

for which the radicand is negative.

It is possible to map general DM parameters to the KNB case, when they are given by the Eq. (2.11). As discussed in Ref. [31], if D_1, D_2 and D_3 are the solution of the flat-band constraint given in the Eqs. (3.18)-(3.22), they can be induced by the KNB mechanism with the following magnitude and angle of the electric field and bond angle θ ,

$$\begin{aligned} E &= \pm \frac{2|D_1|}{|a|} \sqrt{\frac{D_1^2 - a^2 D_2 D_3}{4D_1^2 - a^2(D_2 + D_3)^2}}, \\ \phi &= \arctan\left(\frac{\text{sign}(D_3 + D_2)}{|a|(D_3 - D_2)} \sqrt{4D_1^2 - a^2(D_2 + D_3)^2}\right), \\ \theta &= \arctan\frac{\sqrt{4D_1^2 - a^2(D_2 + D_3)^2}}{|a|(D_2 + D_3)|}. \end{aligned} \quad (3.24)$$

Here the ratio a of the KNB constants for the basal line and zigzag bond of the lattice is arbitrary, and the only additional condition for the mapping is [31]

$$4D_1^2 - a^2(D_2 + D_3)^2 > 0. \quad (3.25)$$

IV. ELECTRIC-FIELD INDUCED FLAT BAND IN THE DISTORTED SAWTOOTH CHAIN

Let us first check the cases of special directions of the electric field, which were considered previously for symmetric sawtooth chain in Ref. [30]. There a remarkable result was obtained for the field parallel to the basal line (see Eq. (1.2)), in which case no further constraints for the coupling constants are needed. Although one might expect similar features in the distorted chain as well, the situation turns out to be different. Namely for this specific case of an electric field $\mathbf{E} = (E, 0, 0)$, the flat-band conditions immediately lead to the following DM parameters,

$$\begin{aligned} D_1 &= 0, \\ D_2 &= -E \sin \theta_1, \\ D_3 &= E \sin \theta_2. \end{aligned} \quad (4.26)$$

Then a flat band results if the electric field has the magnitude and a symmetric exchanges have an appropriate ratio,

$$\begin{aligned} E &= \pm \frac{1}{\sin \theta_2} \left[J_1^2 \left(\frac{\sin^2 \theta_2}{\sin^2 \theta_1} + 2 \text{sign}(J_1) \Delta_1 \frac{\sin \theta_2}{\sin \theta_1} + 1 \right) - J_2^2 \frac{\sin^2 \theta_2}{\sin^2 \theta_1} \right]^{\frac{1}{2}}, \\ J_3 &= \frac{\sin \theta_2}{\sin \theta_1} J_2. \end{aligned} \quad (4.27)$$

Thus, the remarkable result of Ref. [30] can be reproduced here only when $\theta_2 = \theta_1$ and $J_3 = J_2$, i.e., in the case of a non-distorted and symmetric sawtooth chain. The fact that the this electric-field driven flat band requires $J_3 = J_2$ was found also in Ref. [31]. Hence in general an additional constraint is needed, which was absent in the result of Ref. [30] for $\phi = 0$ only because $J_3 = J_2$ was assumed at the outset. For the corresponding saturation field given in Eq. (3.17) we find

$$\begin{aligned} B_0 &= \frac{J_1}{2} \left(2\Delta_1 + \frac{\sin^2 \theta_1 + \sin^2 \theta_2}{\sin \theta_1 \sin \theta_2} \right) \\ &\quad + \frac{J_2}{2} \left(\Delta_2 + \frac{\sin \theta_2}{\sin \theta_1} \Delta_3 \right), \end{aligned} \quad (4.28)$$

which reduces to the known results for the non-distorted sawtooth chain if $\theta_2 = \theta_1$ and $J_3 \Delta_3 = J_2 \Delta_2$ [30, 31], namely

$$B_0^{(0)} = J_1(1 + \Delta_1) + J_2 \Delta_2. \quad (4.29)$$

The saturation magnetisation has a non-monotonous dependence on the distorted bond angle θ_2 . For positive values of J_1 it has a maximum at $\theta_2 = \frac{\pi}{2}$ and minima at

$$\theta_2 = \left| \arcsin \left(\frac{\sqrt{J_1} \sin \theta_1}{\sqrt{J_1 + J_2 \Delta_3}} \right) \right|. \quad (4.30)$$

Interestingly there is no dependence on θ_1 in the saturation field in this case,

$$\begin{aligned} B_0 &= \frac{J_1}{2} \left(2\Delta_1 \pm \frac{2J_1^2 + J_2 \Delta_3}{\sqrt{J_1(J_1 + J_2 \Delta_3)}} \right) \\ &\quad + \frac{J_2}{2} \left(\Delta_2 \pm \frac{\sqrt{J_1}}{\sqrt{J_1 + J_2 \Delta_3}} \Delta_3 \right). \end{aligned} \quad (4.31)$$

It is also interesting to consider the case of small distortions, $\theta_2 = \theta_1 + \delta$, where $|\delta| \ll \theta_1$. In this case the saturation field depends on δ in leading order as (for $\Delta_3 = \Delta_2$)

$$B_0 \simeq B_0^{(0)} + \frac{1}{2} J_2 \Delta_2 \cot \theta_1 \cdot \delta. \quad (4.32)$$

In Ref. [30], an electric field pointing parallel to the zigzag bond, $\phi = \theta$, for the non-distorted sawtooth chain. In

contrast to the previous case $\phi = 0$ an additional constraint similar to the distorted case appeared,

$$\begin{aligned} E &= \pm \frac{2\sqrt{\cos^2 \theta - a^2}}{a^2 \sin \theta} |J_1|, \\ J_2 &= J_3 = \frac{2 \cos \theta}{a} J_1. \end{aligned} \quad (4.33)$$

To generalize this result to the distorted sawtooth case we choose the direction of the electric field parallel to the left side of triangles, $\phi = \theta_1$, which leads to the following configuration of the DM parameters:

$$\begin{aligned} D_1 &= aE \sin \theta_1, \\ D_2 &= 0, \\ D_3 &= E \sin (\theta_1 + \theta_2). \end{aligned} \quad (4.34)$$

The flat-band value of the electric-field magnitude and the additional constraint for the exchange couplings are then

$$\begin{aligned} E &= \pm \frac{1}{\sin (\theta_1 + \theta_2)} \left[J_2^2 \left(\frac{\sin^2 (\theta_1 + \theta_2)}{a^2 \sin^2 \theta_1} - 1 \right) \right. \\ &\quad \left. - J_1^2 \frac{\sin^2 (\theta_1 + \theta_2)}{a^2 \sin^2 \theta_1} - 2J_1 |J_2| \Delta_1 \frac{\sin (\theta_1 + \theta_2)}{a \sin \theta_1} \right]^{\frac{1}{2}} \\ J_3 &= \frac{\sin (\theta_1 + \theta_2)}{a \sin \theta_1} J_1. \end{aligned} \quad (4.35)$$

The saturation field then takes the following form,

$$\begin{aligned} B_0 &= \frac{J_2}{2} \left(\Delta_2 + \frac{\sin (\theta_1 + \theta_2)}{a \sin \theta_1} \right) \\ &\quad + \frac{J_1 \Delta_3}{2} \frac{\sin (\theta_1 + \theta_2)}{a \sin \theta_1}. \end{aligned} \quad (4.36)$$

It is easy to see that this expression has no local minimum, and it has only a local maximum at $\theta_2 = \theta_1 + \frac{\pi}{2}$. However, the minimal value is reached at $\theta_2 = \frac{\pi}{2}$. We conclude that for given value of θ_1 the maximal possible value of the second angle is $\frac{\pi}{2}$. For $\theta_2 = \frac{\pi}{2}$ the saturation field transforms to

$$B_0 = \frac{J_2}{2} \left(\Delta_2 + \frac{\cot \theta_1}{a} \right) + \frac{J_1 \Delta_3}{2} \frac{\cot \theta_1}{a}. \quad (4.37)$$

In the limit of small distortion this becomes

$$B_0 \simeq B_0^{(0)} + (J_2 + J_1 \Delta_3) \frac{\cos (2\theta_1)}{\sin \theta_1} \cdot \delta, \quad (4.38)$$

where

$$B_0^{(0)} = \frac{J_2}{2} \left(\Delta_2 + \frac{2 \cos \theta_1}{a} \right) + \frac{J_1 \Delta_3}{2} \frac{2 \cos \theta_1}{a} \quad (4.39)$$

is the saturation field for the non-distorted case [30, 31]. The situation when the electric field is parallel to the right sides of the triangle ($\phi = -\theta_2$ or $\phi = \pi - \theta_2$) is very

similar, the flat-band value of electric field can be obtained from Eqs. (4.35)-(4.39) by switching J_2 and J_3 and θ_1 and θ_2 . To conclude, the result obtained in Ref. [30] concerning the electric-field driven flat band without an additional condition for the exchange coupling constant was accidental in the sense that the couplings were chosen symmetric throughout, whereas this follows in the more general case from Eq. (4.27). However, as shown in Ref. [31], one can nevertheless pick a direction of the electric field which is not necessarily parallel to the lattice bonds and then adjust the magnitude of electric field to drive the system into the flat-band regime. For this one starts from the flat band constraints in terms of D_1, D_2, D_3 in Eqs. (3.18)-(3.23) and constructs a one-parameter family of mappings

$$f_a : \begin{pmatrix} D_1 \\ D_2 \\ D_3 \end{pmatrix} \rightarrow \begin{pmatrix} \phi \\ E \\ \theta \end{pmatrix}, \quad (4.40)$$

where the ratio a of KNB constants plays the role of a free parameter. Thus, for given DM constants which correspond to a flat band in the general sawtooth chain, flat band induced by the KNB mechanism can be obtained from the electric field angle and magnitude and the bond angle as functions of (D_1, D_2, D_3) and of the parameter a . These functions are given in Eq. (3.24). For the distorted sawtooth chain the mapping is more complicated and the second, distorted angle θ_2 plays the role of an additional parameter, giving rise to a broader family of possible KNB realizations of the given solution of the flat band constraints. However, due to the symmetry of the KNB-induced DM parameters, there is an invariance under $\theta_1 \leftrightarrow \theta_2$ and $D_2 \leftrightarrow D_3$, i.e., the mapping where θ_1 is a parameter instead of θ_2 has a similar structure with D_2 and D_3 interchanged,

$$\begin{aligned} g_{a, \theta_2} : \begin{pmatrix} D_1 \\ D_2 \\ D_3 \end{pmatrix} &\rightarrow \begin{pmatrix} \phi \\ E \\ \theta_1 \end{pmatrix}, \\ g_{a, \theta_1} : \begin{pmatrix} D_1 \\ D_2 \\ D_3 \end{pmatrix} &\rightarrow \begin{pmatrix} \phi \\ E \\ \theta_2 \end{pmatrix}, \end{aligned} \quad (4.41)$$

where

$$g_{a, \theta_1} \circ P_{23} = g_{a, \theta_2}, \quad P_{23} : \begin{pmatrix} D_1 \\ D_2 \\ D_3 \end{pmatrix} = \begin{pmatrix} D_1 \\ D_3 \\ D_2 \end{pmatrix}. \quad (4.42)$$

Let us illustrate this mapping for the example of the second case, when the left angle θ_2 is expressed by the DM parameters and by the right angle θ_1 , i.e., $\theta_2 = \theta_2(D_1, D_2, D_3, a, \theta_1)$, so that the angle θ_1 plays the role of a free parameter here. From Eq. (2.12) we find

$$D_2 \sin \theta_2 + D_3 \sin \theta_1 = \frac{D_1}{a} \sin (\theta_1 + \theta_2) \quad (4.43)$$

which can be solved with respect to $\sin \theta_2$,

$$\begin{aligned} & \theta_2(D_1, D_2, D_3, a, \theta_1) \\ &= \arcsin \frac{\text{sign}(a) D_1 \sin \theta_1}{\sqrt{D_1^2 + a^2 D_2^2 - 2aD_1 D_2 \cos \theta_1}} \\ & \quad - \arcsin \frac{|a| D_3 \sin \theta_1}{\sqrt{D_1^2 + a^2 D_2^2 - 2aD_1 D_2 \cos \theta_1}}. \end{aligned} \quad (4.44)$$

Combining the expressions for D_2 and D_3 from Eqs. (2.12) and (4.43), one can then express angle and magnitude of the electric field

$$\begin{aligned} \phi &= \arctan \frac{D_3 \sin \theta_1 + D_2 \sin \theta_2(D_1, D_2, D_3, a, \theta_1)}{D_3 \cos \theta_1 - D_2 \cos \theta_2(D_1, D_2, D_3, a, \theta_1)}, \\ E &= \pm \frac{|D_1|}{|a|} \left[1 + \left(\frac{D_3 \cos \theta_1 - D_2 \cos \theta_2(D_1, D_2, D_3, a, \theta_1)}{D_3 \sin \theta_1 + D_2 \sin \theta_2(D_1, D_2, D_3, a, \theta_1)} \right)^2 \right]. \end{aligned} \quad (4.45)$$

Thus one of the bond angles, θ_1 in this case, plays the role of a continuous parameter which leads to a flat band for given KNB-induced D_1, D_2 and D_3 . Varying θ_1 in Eq. (4.45) not keeps the flat band, but does not even change the values of the DM parameters. Let us exhibit two examples of this mapping, obtained in Ref. [31], both with $J_1 = 1, J_2 = 1, J_3 = 3, \Delta_1 = \Delta_2 = \Delta_3 = 1, D_1 = 1, D_2 = -2, D_3 = -1$, and two distinct values of the right bond angle, $\theta_1 = \frac{\pi}{8}$ and $\theta_1 = \frac{\pi}{2}$, which both correspond to the same Hamiltonian (2.3). The parameters of the electric field and the left bond angle are nevertheless different,

$$\begin{aligned} \theta_1 &= \frac{\pi}{8}, \quad \theta_2 = 2 \arcsin \left[\frac{\sin \frac{\pi}{8}}{\sqrt{5 - 4 \cos \frac{\pi}{8}}} \right], \\ \phi &= \arctan \frac{(5 - 4 \cos \frac{\pi}{8})(\sin \frac{\pi}{8} - 2 \sin \theta_2)}{3(2 - \cos \frac{\pi}{8})}, \\ E &= \pm \frac{\sqrt{5 + 4 \cos(\frac{\pi}{8} + \theta_2)}}{|\sin \frac{\pi}{8} - 2 \sin \theta_2|}, \end{aligned} \quad (4.46)$$

and

$$\begin{aligned} \theta_1 &= \frac{\pi}{4}, \quad \theta_2 = 2 \arcsin \left(\frac{1}{\sqrt{10 - 4\sqrt{2}}} \right), \\ \phi &= \arctan \frac{17(\sqrt{2} - 4 \sin \theta_2)}{48 + 9\sqrt{2}}, \\ E &= \pm \sqrt{1 + \left(\frac{1 + 2\sqrt{2} \cos \theta_2}{1 - 2\sqrt{2} \sin \theta_2} \right)^2} \end{aligned} \quad (4.47)$$

Interestingly, the solution with $\theta_1 = \frac{\pi}{3}$ corresponds to a non-distorted sawtooth chain,

$$\theta_1 = \frac{\pi}{3}, \quad \theta_2 = \frac{\pi}{3}, \quad \phi = -\frac{\pi}{6}, \quad E = \pm 2. \quad (4.48)$$

These three sets of the parameters for the sawtooth chain with KNB parameters all realize the same physical picture. To illustrate this we calculated the zero-temperature magnetization curves by exact diagonalization (see Fig. 2). For a magnetic field below saturation, the localized magnons of the flat bands lower the energy of the system according to Eq. (3.16). Thus, a magnon crystal forms instantly during the magnetization process giving rise to a magnetization plateau at half the saturated magnetization equal. However, at $B = B_0$ this magnon crystal becomes degenerate with the saturated fully polarized spin configuration. This leads to a magnetization jump from the $M = \frac{1}{2}$ to the $M = 1$ plateau. This magnetization profile is typical for systems with localized magnons [1, 25–27] and also observed in the Fig. 2. An additional plateau at $M = 0$ is in fact independent of the flat band and rather indicates the spin-liquid ground state which is inherent to the sawtooth chain with DM interactions [57].

V. SUMMARY

In the present paper we presented further analysis of the solutions of flat-band constraints for the a generalized sawtooth chain model with DM interactions. Our main focus was the mapping of the general solution in terms of DM constants to the case when the effective DM interaction is generated by the KNB mechanism of spin-induced ferroelectricity, which is sensitive to the geometry. In contrast to our previous results given in Refs. [30] and [31], here we considered distorted sawtooth chain featuring two distinct bond angles at the base of the tri-

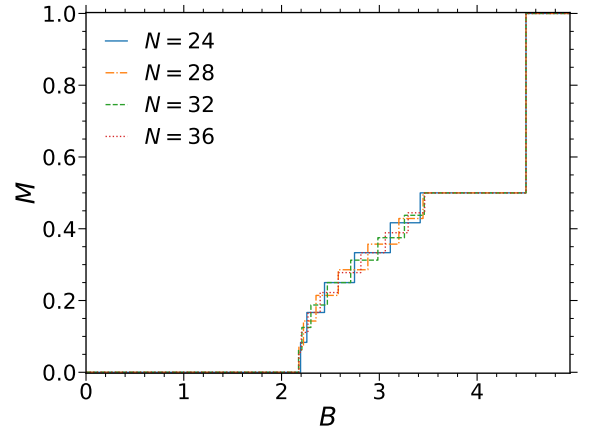


FIG. 2. (Color online) Zero-temperature exact diagonalization results for the magnetization in the distorted sawtooth chain with KNB mechanism for the values of electric field magnitude, angle, θ_1, θ_2 given in the Eqs. (4.46)-(4.48). All three sets of parameters lead to the same magnetization curve as they all correspond to the same Hamiltonian (2.3), namely $J_1 = 1, J_2 = 1, J_3 = 3, \Delta_1 = \Delta_2 = \Delta_3 = 1$ and $D_1 = 1, D_2 = -2, D_3 = -1$.

angles. The distortion is related to the modification of relations linking DM parameters with the electric field characteristics, magnitude and direction. We considered in particular a electric field parallel to the lattice bonds. For each cases we found the corresponding values of the electric field driving the one-magnon spectrum into a flat band mode. The behavior of the saturation magnetic field, particularly its dependence on the distorted angle, was also analyzed. As a main result we constructed the mapping from the general solution of the flat band constraints, given in terms of general DM parameters, into the electric-field driven flat-band constraints, by expressing electric field magnitude, angle and one of the bond

angles in terms of D_1 , D_2 , and D_3 .

ACKNOWLEDGEMENTS

V.O. is grateful to the Center for Electronic Correlations and Magnetism for the hospitality during his visits to the University of Augsburg; he and L.A. also acknowledge partial financial support from ANSEF (Grants No. PS-condmatth-3273) and CS RA MESCS (Grants No. 21AG-1C047). V.O. and M.K. acknowledge partial funding by Deutsche Forschungsgemeinschaft (DFG, German Research Foundation) – TRR360 – 492547816.

-
- [1] O. Derzhko, J. Richter, and M. Maksymenko, *Int. J. Mod. Phys. B* **29**, 1530007 (2015).
 - [2] D. Leykam, A. Andreanov, and S. Flach, *Adv. Phys.: X* **3**, 1473052 (2018).
 - [3] J.-H. Bae, T. Sedrakyan, and S. Maltl, *SciPost Phys.* **15**, 139 (2023).
 - [4] S. Lee, A. Andreanov, T. Sedrakyan, and S. Flach, *Phys. Rev. B* **109**, 245137 (2024).
 - [5] A. Mallick and A. Andreanov, *Phys. Rev. B* **111**, 014201 (2025).
 - [6] B. Sutherland, *Phys. Rev. B* **34**, 5208 (1986).
 - [7] A. Mielke, *J. Phys. A: Math. Gen.* **24**, L73 (1991).
 - [8] H. Tasaki, *Phys. Rev. Lett.*, **69**, 1608 (1992).
 - [9] A. Mielke and H. Tasaki, *Commun. Math. Phys.*, **158**, 341 (1993).
 - [10] H. Tasaki, *Prog. Theor. Phys.* **99**, 489 (1998).
 - [11] O. Derzhko, J. Richter, A. Honecker, M. Maksymenko, and R. Moessner, *Phys. Rev. B* **81**, 014421 (2010).
 - [12] M. Maksymenko, A. Honecker, R. Moessner, J. Richter, and O. Derzhko, *Phys. Rev. Lett.*, **109**, 096404 (2012).
 - [13] V. Baliha, J. Richter, and O. Derzhko, *Acta Phys. Pol. A* **132**, 1256 (2017).
 - [14] D. Leykam, and S. Flach, *APL Photon.* **3**, 070901 (2018).
 - [15] Jing Yang, Yuanzhen Li, Yumeng Yang, Xinrong Xie, Zijian Zhang, Jiale Yuan, Han Cai, Da-Wei Wang, and Fei Gao, *Nat. Commun.* **15**, 1484 (2024).
 - [16] S. Eyvazi, E. A. Mamonov, R. Heilmann, J. Cuerda, and P. Törmä, *ACS Photonics*, **12**, 1570 (2025).
 - [17] Sh. Taie, H. Ozawa, T. Ichinose, T. Nishio, Sh. Nakajima, and Y. Takahashi, *Sci. Adv.* **1**, e1500854 (2015).
 - [18] H. Ozawa, Sh. Taie, T. Ichinose, and Y. Takahashi, *Phys. Rev. Lett.* **118**, 175301 (2017).
 - [19] Sh. Taie, T. Ichinose, H. Ozawa, and Y. Takahashi, *Nat. Commun.* **11**, 1 (2020).
 - [20] Zhihao Jiang, K. Hsieh, A. J. H. Jones, P. Majchrzak, S. Chakradhar, K. Watanabe, T. Taniguchi, J. A. Miwa, Yong P Chen, and S. Ulstrup, *2D Mater.* **10**, 045027 (2023).
 - [21] Zhen-Yu Wang, Jia-Jun Ma, Qianqian Chen, Kefan Wu, Shuigang Xu, Qing Dai, Zheng Zhu, Jindong Ren, Hong-Jun Gao, and Xiao Lin, *Nanoscale* **16**, 18852 (2024).
 - [22] J. G. Checkelsky, B. A. Bernevig, P. Coleman, Q. Si, and S. Paschen, *Nat. Rev. Mater.* **9**, 509 (2024).
 - [23] F. Garmroudi, J. Coulter, I. Serhienko, S. Di Cataldo, M. Parzer, A. Riss, M. Grasser, S. Stockinger, S. Khmelevskiy, K. Pryga, B. Wiendlocha, K. Held, T. Mori, E. Bauer, A. Goerges, and A. Pustogow, *Phys. Rev. X* **15**, 021054 (2025).
 - [24] D. A. Abanin, E. Altman, I. Bloch, and M. Serbyn, *Rev. Mod. Phys.* **91**, 021001 (2019).
 - [25] J. Schulenburg, A. Honecker, J. Schnack, J. Richter, and H.-J. Schmidt, *Phys. Rev. Lett.* **88**, 167207 (2002).
 - [26] J. Richter, J. Schulenburg, A. Honecker, J. Schanck, and H.-J. Schmidt, *J. Phys.: Condens. Matter* **16**, S779 (2004).
 - [27] J. Richter, *Low Temp. Phys.* **31**, 695 (2005).
 - [28] M. E. Zhitomirsky, H. Tsunetsugu, *Phys. Rev. B* **70**, 100403(R) (2004).
 - [29] O. Derzhko and J. Richter, *Phys. Rev. B* **70**, 104415 (2004).
 - [30] J. Richter, V. Ohanyan, J. Schulenburg, and J. Schnack, *Phys. Rev. B* **105**, 054420 (2022).
 - [31] V. Ohanyan, J. Richter, M. Sekania, L. Giambattista, A. Andreanov, and M. Kollar, *On flat bands in $J_1-J_2-J_3$ sawtooth chain*, arXiv:2511.15461 (2025).
 - [32] H. Katsura, N. Nagaosa, and A. V. Balatsky, *Phys. Rev. Lett.* **95**, 057205 (2005).
 - [33] C. Jia, S. Onoda, N. Nagaosa, and J. H. Han, *Phys. Rev. B* **74**, 224444 (2006).
 - [34] I. Solov'yev, R. Ono, and S. Nikolaev, *Phys. Rev. Lett.* **127**, 187601 (2021).
 - [35] I. V. Solov'yev, *Condens. Matter* **10**, 21 (2025).
 - [36] A. Metavitsiadis, C. Psaroudaki, and W. Brenig, *Phys. Rev. B* **101**, 235143 (2020).
 - [37] T. Hutak, T. Krokhmalkii, O. Derzhko, and J. Richter, *Eur. Phys. J. B* **96**, 50 (2023).
 - [38] F. Johannesmann, J. Ecksele, H. Schlüter, and J. Schnack, *Phys. Rev. B* **108**, 064304 (2023).
 - [39] R. Rausch, M. Peschke, C. Plorin, J. Schnack, and C. Karrasch, *SciPost Phys.* **14**, 052 (2023).
 - [40] N. Reichert, H. Schlüter, T. Heitmann, J. Richter, R. Rausch, and J. Schnack, *Z. Naturforsch. A* **79**, 283 (2024).
 - [41] R. Rausch and C. Karrasch, *Phys. Rev. B* **111**, 045154 (2025).
 - [42] M. Brockmann, A. Klümper, and V. Ohanyan, *Phys. Rev. B* **87**, 054407 (2013).
 - [43] W.-L. You, G.-H. Liu, P. Horsch, and A. M. Oleś, *Phys. Rev. B* **90**, 094413 (2014).
 - [44] O. Menchysyn, V. Ohanyan, T. Verkholyak, T. Krokhmalkii, and O. Derzhko, *Phys. Rev. B*

- 92**, 14427 (2015).
- [45] P. Thakur and P. Durganandini, Phys. Rev. B **97**, 064413 (2018).
 - [46] J. Sznajd, Phys. Rev. B **97**, 214410 (2018).
 - [47] T.-Ch. Yi, W.-L. You, N. Wu, and A. M. Oleś, Phys. Rev. B **100**, 024423 (2019).
 - [48] J. Sznajd, J. Magn. Magn. Mater. **479**, 254 (2019).
 - [49] V. Ohanyan, Condens. Matter Phys. **23**, 43704 (2020).
 - [50] O. Baran, Ukr. J. Phys. **66**, 890 (2021).
 - [51] O. Baran, V. Ohanyan, and T. Verkholyak, Phys. Rev. B **98**, 064415 (2018).
 - [52] N. Avalishvili, G. I. Japaridze, and G. L. Rossini, Phys. Rev. B **99**, 205159 (2019).
 - [53] G. I. Japaridze, H. Cheraghi, and S. MahdaviFar, Phys. Rev. E **104**, 014134 (2021).
 - [54] N. Esaki, Y. Akagi, and H. Katsura, Phys. Rev. Res. **6**, L032050 (2024).
 - [55] W. Brenig, Phys. Rev. B **112**, 115132 (2025).
 - [56] W. Brenig, *Two-dimensional nonlinear dynamical response of the magnetoelectrically driven dimerized spin-1/2 chain*, arXiv:2507.17823 (2025).
 - [57] Zhihao Hao, Yuan Wan, I. Rousochatzakis, J. Wildeboer, A. Seidel, F. Mila, and O. Tchernyshyov, Phys. Rev. B **84**, 094452 (2011).